Available online at www.sciencedirect.com
SCIENCE DIRECT®
Polymer 45 (2004) 367–378
polymer
www.elsevier.com/locate/polymer

Micelles of polyisobutylene-*block*-poly(methacrylic acid) diblock copolymers and their water-soluble interpolyelectrolyte complexes formed with quaternized poly(4-vinylpyridine)

Dmitry V. Pergushov[a,*], Ekaterina V. Remizova[a], Michael Gradzielski[b], Peter Lindner[c], Jesper Feldthusen[d], Alexander B. Zezin[a], Axel H.E. Müller[e,*], Victor A. Kabanov[a]

[a]*Department of Polymer Science, School of Chemistry, Moscow State University, Vorob'evy Gory, 119992 Moscow, Russian Federation*
[b]*Physikalische Chemie I, Universität Bayreuth, D-95440 Bayreuth, Germany*
[c]*Institut Max von Laue-Paul Langevin, F-38042 Grenoble Cedex 9, France*
[d]*Institut für Physikalische Chemie, Universität Mainz, D-55099 Mainz, Germany*
[e]*Makromolekulare Chemie II and Bayreuther Zentrum für Kolloide und Grenzflächen, Universität Bayreuth, D-95440 Bayreuth, Germany*

Received 21 April 2003; received in revised form 22 October 2003; accepted 29 October 2003

Abstract

The micellization of ionic amphiphilic diblock copolymers, polyisobutylene-*block*-poly(methacrylic acid) (PIB-*b*-PMAA), with a constant degree of polymerization of the non-ionic block ($\overline{DP}_n = 20$) and various degrees of polymerization of the polyelectrolyte block ($\overline{DP}_n = 100-425$) was examined in aqueous media by means of fluorescence spectroscopy using pyrene as a polarity probe. The molar values of the critical micellization concentration (cmc) were found to be around 2×10^{-6} mol/l, being nearly independent of the length of the polyelectrolyte block as well as pH (in the range 6–9) and ionic strength (≤ 0.5 M NaCl) while the specific cmc values varied from 20 to 100 mg/l. Small-angle neutron scattering (SANS) and dynamic light scattering (DLS) experiments provided evidence that aggregation numbers and hydrodynamic radii of the formed copolymer micelles are sensitive to variations of pH and ionic strength, indicating that these micelles might be 'dynamic' rather than 'frozen' ones. It was also shown by means of a combination of turbidimetry, analytical ultracentrifugation, fluorescence spectroscopy, SANS, and DLS that the formed copolymer micelles mixed with a strong cationic polyelectrolyte, poly(*N*-ethyl-4-vinylpyridinium bromide) at charge ratio $Z = [+]/[-]$ not exceeding a certain critical value $Z_M < 1$, generate peculiar water-soluble micellar complex onion-like species, each containing a two-phase hydrophobic nucleus and a hydrophilic corona. The nucleus consists of a PIB core and a shell assembled from the fragments of water-insoluble interpolyelectrolyte complex. The corona is formed by the excess fragments of poly(sodium methacrylate) blocks not involved in complexation with poly(*N*-ethyl-4-vinylpyridinium bromide).

Keywords: Ionic amphiphilic diblock copolymers; Micelles; Interpolyelectrolyte complexes

1. Introduction

It is well known that self-assembly of ionic amphiphilic block copolymers in aqueous solutions results in the formation of micelles, each micelle consisting of a compact hydrophobic core built up from non-polar blocks and a swollen hydrophilic corona formed by polyelectrolyte blocks. Such macromolecular assemblies are of considerable interest not only from a fundamental point of view but also because of their numerous promising potential applications, e.g. as reagents for removal of non-polar pollutants from water, stabilizers in emulsion polymerization, containers for targeted drug delivery, nanoreactors, etc. The micellization of ionic amphiphilic block copolymers as well as the structure of their micelles have been intensively investigated during the past decades. The main results of these studies have been exhaustively reviewed in Refs. [1–3].

Most of the work on ionic amphiphilic block copolymers dealt with those containing polystyrene as a non-polar block. Because of a relatively high glass transition

* Corresponding authors. Fax: +7-95-939-01-74. + 49-921-55-3393 (A.H.E. Müller).
E-mail addresses: pergush@genebee.msu.su (D.V. Pergushov), axel.mueller@uni-bayreuth.de (A.H.E. Müller).

0032-3861/$ - see front matter © 2004 Elsevier Ltd. All rights reserved.
doi:10.1016/j.polymer.2003.10.086

temperature of polystyrene ($T_g \approx 105$ °C), a transfer of such copolymers into aqueous media is usually a complicated procedure requiring either a long heating at about 100 °C or a stepwise dialysis from a suitable organic solvent miscible with water (e.g. tetrahydrofuran, dioxane, dimethylformamide). After cooling or removal of the organic solvent, so-called 'frozen' micelles are generated, such micelles being unable to exchange unimers, i.e. single block copolymer molecules. The structure and the properties of such macromolecular assemblies were thoroughly studied by a number of research groups (cf. references in the reviews [1–3]).

Recently, a novel approach to the synthesis of yet unexplored ionic amphiphilic diblock copolymers with polyisobutylene as a very hydrophobic block via a combination of living cationic and anionic polymerizations has been developed [4,5]. Since polyisobutylene has a low glass transition temperature ($T_g \approx -65\,°C$), such copolymers can be easily dissolved in water without being heated over a long period of time or stepwise dialysis from organic into aqueous media. The micelles formed by these copolymers might be expected to be 'dynamic', that is, being able to exchange unimers.

The aggregation behavior of polyisobutylene-*block*-poly(methacrylic acid) diblock copolymers consisting of the hydrophobic block and the polyelectrolyte block of comparable lengths as well as the structure of their assemblies were examined earlier [5]. In this work, we have studied the micellization of similar diblock copolymers but containing relatively short polyisobutylene block and much longer poly(methacrylic acid) block as well as the structure of the formed micelles. Because the coronas of such assemblies are built up from ionic blocks which can, in fact, form interpolyelectrolyte complexes (IPECs) with oppositely charged macromolecules, we have also examined the complexation of polyisobutylene-*block*-poly(methacrylic acid) micelles with a strong cationic polyelectrolyte, poly(*N*-ethyl-4-vinylpyridinium bromide).

Previously, block copolymers consisting of ionic and hydrophilic non-ionic blocks were approached for a synthesis of IPECs. The complexation of such copolymers with oppositely charged macromolecules was demonstrated to result in the formation of micellar species containing a water-insoluble IPEC core fringed with a corona built up from non-ionic hydrophilic blocks [6–11]. In contrast to those studies, the ionic amphiphilic diblock copolymers used in this work as starting materials for a preparation of IPECs are already present in the system as micelles, each containing a hydrophobic core fringed with a polyelectrolyte corona. Some of our first results on interpolyelectrolyte complexation in such systems and the properties of the resulting IPECs have been very recently reported elsewhere [12].

2. Experimental part

2.1. Materials

Polyisobutylene-*block*-poly(*tert*-butyl methacrylate) diblock copolymers (PIB-*b*-P*t*BMA$_x$) with a constant degree of polymerization of the PIB block ($\overline{DP}_n = 20$) and different degrees of polymerization of the P*t*BMA block (the subscript x denotes $\overline{DP}_n$ of the P*t*BMA block) were synthesized via a combination of living cationic and anionic polymerizations as described elsewhere [4,5]. The molecular weight distributions of the PIB precursor (measured separately) and PIB-*b*-P*t*BMA$_x$ were determined by means of size exclusion chromatography (SEC) with the use of PIB and P*t*BMA standards. For the diblock copolymers, a weighted average of the homopolymer calibration curves were used. SEC was performed using PSS SDV-gel columns (5 μm, 60 cm, 1 × linear(10^2–10^5 Å), 1 × 100 Å) with THF as eluent at a flow rate of 1.0 ml/min at room temperature using UV ($\lambda = 230$ and 260 nm) and RI detection. In order to prepare polyisobutylene-*block*-poly(methacrylic acid) diblock copolymers (PIB-*b*-PMAA$_x$), the *tert*-butyl methacrylate groups of PIB$_{20}$-*b*-P*t*BMA$_x$ were hydrolyzed with hydrochloric acid in dioxane at 80 °C. The molecular characteristics of the prepared PIB-*b*-PMAA$_x$ are given in Table 1.

Poly(*N*-ethyl-4-vinylpyridinium bromide) (PVP·EtBr) was synthesized from poly(4-vinylpyridine) (Polysciences Inc.) with $\bar{M}_w = 50,000$ g/mol ($\overline{DP}_w \cong 480$; polydispersity of the sample is not specified by the supplier) via its exhaustive quaternization with a 10-fold excess of ethyl bromide at 60 °C. As determined by ^{1}H NMR spectroscopy, the molar fraction of quaternized pyridine units in the resulting polymer was close to 0.9, corresponding to about 430 charged monomer units per polymer chain.

2.2. Preparation of stock solutions of polymers

Stock solutions of PIB$_{20}$-*b*-PMAA$_x$ were prepared by dissolving the copolymers in water containing a desired amount of NaOH (Riedel-de Haën) at 50–60 °C under continuous stirring. The concentration of carboxylic groups in the resulting stock copolymer solutions was 0.1 M. The pH of the stock solutions of PIB$_{20}$-*b*-PMAA$_x$ was precisely adjusted to a final desired value by adding 1 M HCl or 1 M

Table 1
Molecular characteristics of the amphiphilic diblock copolymers; $\bar{M}_n$ (PIB) = 1100 g/mol[a]

Sample	ϕ_{IB}[b]	$\bar{M}_n$ (PMAA)	$\bar{M}_n$ (PMANa)	$\bar{M}_w/\bar{M}_n$
PIB$_{20}$-*b*-PMAA$_{100}$	0.167	8,800	11,050	1.16
PIB$_{20}$-*b*-PMAA$_{280}$	0.067	24,200	30,400	1.10
PIB$_{20}$-*b*-PMAA$_{425}$	0.045	36,700	46,100	1.20

[a] Polydispersity of the PIB block $\bar{M}_w/\bar{M}_n = 1.09$.
[b] Molar fraction of isobutylene monomer units.

NaOH. A stock solution of PVP·EtBr was prepared by dissolving the cationic polyelectrolyte in water. The concentration of pyridinium groups in the resulting stock solution of PVP·EtBr was 0.05 M.

2.3. Methods

2.3.1. Fluorescence spectroscopy

Sample solutions of PIB_{20}-*b*-$PMAA_x$ for fluorescence measurements were prepared by an appropriate dilution of the stock copolymer solutions with the corresponding buffers: 0.01 M TRIS (2-amino-2-hydroxymethyl-1,3-propanediol, Fluka) with pH 9 and 0.05 M phosphate buffer with pH 8, 7, or 6. The ionic strength of the sample solutions was varied by adding 4 M NaCl (ICN). Sample solutions containing both PIB_{20}-*b*-$PMAA_x$ and PVP·EtBr were obtained by mixing the stock solutions of these polymers in the presence of a certain amount of NaCl, followed by a subsequent dilution of such mixtures with 0.01 M TRIS.

The samples for fluorescence measurements were prepared according to a procedure similar to those described elsewhere [13–15]. Certain aliquots of a solution of pyrene (Aldrich) in acetone were carefully dropped into empty dark vials by a Hamilton microsyringe, acetone was afterwards evaporated by gentle heating. Then the sample solutions were added. To equilibrate pyrene, the prepared samples were kept at 40–50 °C for ca. 2 days under intensive stirring. The final concentration of the fluorescent probe in the prepared samples was kept constant at 5×10^{-7} M, that is, only slightly below the saturation concentration of pyrene in water at 22 °C.

Steady-state fluorescence spectra of the air-equilibrated samples were recorded with a Hitachi F-4000 fluorescence spectrophotometer (right angle geometry, 1 cm × 1 cm quartz cell). The widths of slits were chosen to be 3 and 1.5 nm for excitation and emission, respectively.

2.3.2. Small-angle neutron scattering (SANS)

Sample solutions for SANS experiments were prepared by dissolving PIB_{20}-*b*-$PMAA_x$ in D_2O (Aldrich) containing a desired amount of NaOH (Riedel-de Haën) at 50–60 °C under continuous stirring. The final concentration of the copolymers in the sample solutions was ca. 0.9–1% (wt). In all cases, the prepared solutions were homogeneous, transparent, and of low viscosity. The sample solutions were put into quartz cells with 2 mm path length (Hellma). The degree of neutralization, α, of the PMAA blocks of the copolymers was controlled by the amount of NaOH in the sample solutions. The ionic strength of the sample solutions was adjusted by adding NaCl (Merck).

The SANS measurements were performed using the instruments D11 and D22 of the Institut Max von Laue-Paul Langevin (ILL, Grenoble, France) with neutron wavelengths $\lambda = 6$ and 8 Å, respectively. In the case of D11, sample-to-detector distances 1.1, 4, and 16 m were employed while they were 1.5 and 12 m in the case of D22. In both cases, a total range of the magnitude of the scattering vector, $q = 0.003–0.45$ Å^{-1}, was covered. The detector sensitivity and the intensity of the primary beam were calibrated by a comparison with the scattering from a 1 mm reference sample of water. The obtained data were radially averaged, corrected for the detector background, the detector dead time, and the scattering from an empty cell. Then they were converted into absolute units by a comparison with the scattering from water according to standard routines supplied by the ILL [16]. It should be noted that the SANS curves presented in this paper still contain the incoherent background scattering of the solvent and the sample.

2.3.3. Dynamic light scattering (DLS)

Sample solutions for DLS experiments were obtained by an isoionic 50-fold dilution of the sample solutions prepared for the SANS measurements with corresponding aqueous solutions of NaCl. The prepared sample solutions were afterwards thoroughly filtered by passing at least three times through a Nylon filter (13-HV, Millipore) with 0.45 μm pore size.

The DLS measurements were carried out in sealed cylindrical scattering cells at four scattering angles 30, 60, 90, and 120° with the use of an ALV DLS/SLS-SP 5022F equipment consisting of an ALV-SP 125 laser goniometer, an ALV 5000/E correlator, and a He–Ne laser with the wavelength ($\lambda = 632.8$ nm). The CONTIN algorithm was applied to analyze the obtained correlation functions.

2.3.4. Analytical ultracentrifugation

Sample solutions for analytical ultracentrifugation experiments were obtained by mixing the stock solutions of PIB_{20}-*b*-$PMAA_x$ and PVP·EtBr in the presence of a certain amount of NaCl, followed by a subsequent dilution of such mixtures with 0.01 M TRIS.

The sedimentation experiments were carried out with a Beckman (Spinco, model E) analytical ultracentrifuge equipped with a UV–vis absorption optical detector (Scan mode). The speed of rotor rotation was 48,000 rpm.

2.3.5. Turbidimetric titration

Turbidimetric titrations of solutions of PIB_{20}-*b*-$PMAA_x$ micelles with solutions of PVP·EtBr were carried out in isoionic regime at $\lambda = 500$ nm with a Hitachi 150-20 UV–vis spectrophotometer. At this wavelength, the polymers used do not absorb light, therefore the values of optical density result from light scattering only. The titrations were run under continuous stirring; the time interval between subsequent additions of a titrant was equal to 1 min.

3. Results and discussion

3.1. Micellization of PIB-b-PMAA in aqueous solutions

The photophysical properties of pyrene strongly depend on the polarity of the surrounding medium [17,18]. In particular, the fine structure of the emission spectrum of this fluorophore, especially, the ratio between the intensities of first and third vibrational bands, I_1/I_3, is rather sensitive to the polarity of its local environment: this ratio was demonstrated to decrease if the microenvironment of the fluorescent probe becomes less polar. Therefore the formation of macromolecular micelles in aqueous solutions of amphiphilic block copolymers can be detected by means of fluorescence spectroscopy with the use of pyrene as a polarity probe.

The typical dependencies of I_1/I_3 on the concentration of PIB_{20}-*b*-$PMAA_x$ differing in the lengths of their ionic blocks ($x = 100$, 280, and 425) are shown in Fig. 1. The values of I_1/I_3 remain fairly constant at low concentrations of the copolymers, this ratio being very close to that found for pyrene in the pure solvent ($I_1/I_3 \cong 1.85$). Above a certain concentration of PIB_{20}-*b*-$PMAA_x$, the values of I_1/I_3 demonstrate a pronounced decrease upon the rising concentration of the copolymers. The concentration, determined as the intersection of a tangent to the dependence curve of I_1/I_3 on the PIB_{20}-*b*-$PMAA_x$ concentration at its inflection with a horizontal tangent through points corresponding to low concentrations of PIB_{20}-*b*-$PMAA_x$ (the tangents are shown in Fig. 1 as the dashed lines) can be considered as the critical micellization concentration (cmc, indicated with an arrow in Fig. 1). For all copolymers, the molar values of the cmc are evaluated to be around 2×10^{-6} M (the corresponding specific cmc values vary from 24 to 100 mg/l). These values are comparable to those found for polystyrene-*block*-poly(sodium acrylate) diblock copolymers (PS-*b*-PANa) with lengths of hydrophobic and polyelectrolyte blocks similar to those of the corresponding blocks of PIB_{20}-*b*-$PMAA_x$ [14,15]. However, as expected, the determined values are much higher than the values of the cmc obtained for PIB_{70}-*b*-$PMAA_x$ ($x = 52, 70$) and PIB_{134}-*b*-$PMAA_x$ ($x = 145, 288$), i.e. for copolymers with considerably longer hydrophobic blocks. Indeed, values of the cmc for those copolymers were evaluated to be in the range of 10^{-9}–10^{-8} M (<0.3 mg/l) [5].

Fig. 2a shows that the variation of pH from 9 to 6, which according to the obtained potentiometric titration curves (the data are not shown) corresponds to a change of the degree of neutralization of the PMAA blocks from ca. 0.9 to ca. 0.4, is not accompanied by distinct changes of the cmc values of PIB_{20}-*b*-$PMAA_x$. (It should be noted that at pH <6 the reference linear homopolyelectrolyte PMAA ($\overline{DP}_n = 400$) demonstrated a distinct ability to solubilize pyrene. This fact does not allow us to apply the considered fluorescence technique for a determination of the cmc's for PIB_{20}-*b*-$PMAA_x$ under such experimental conditions.) Additionally, an increase of the ionic strength (at least, up to 0.5 M NaCl) does not change the cmc of PIB_{20}-*b*-$PMAA_x$ either (Fig. 2b). Latter is in contrast to low molecular weight ionic surfactants for which a pronounced decrease of the cmc values upon increasing ionic strength in their aqueous solutions is typically observed [19]. These findings suggest that the micellization process in our systems is dominated by the hydrophobicity of the PIB blocks. However,

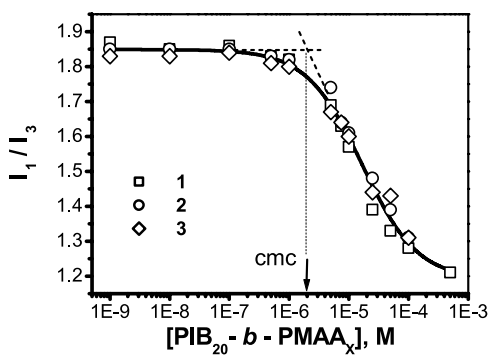

Fig. 1. Dependence of the ratio I_1/I_3 on the concentration of PIB_{20}-*b*-$PMAA_x$ with $x = 100$ (1), 280 (2), and 425 (3); 0.05 M NaCl, pH 9 (0.01 M TRIS); the excitation wavelength is 333 nm, $T = 25$ °C.

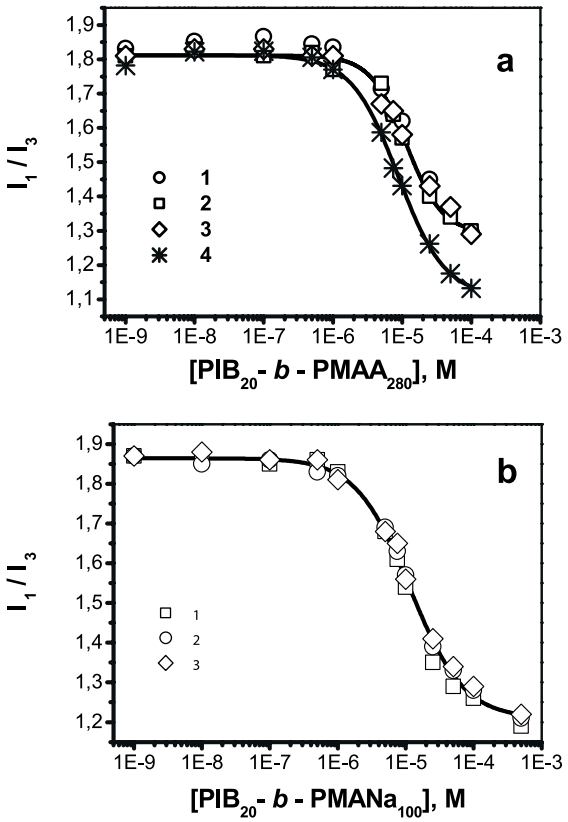

Fig. 2. Dependence of the ratio I_1/I_3 on the concentration of PIB_{20}-*b*-$PMAA_x$ at different values of pH and ionic strength of the surrounding medium; (a) $x = 280$ at 0.05 M NaCl and pH 9 (1), 8 (2), 7 (3), and 6 (4), respectively; (b) $x = 100$ at pH 9 without added NaCl (1), 0.05 M NaCl (2), and 0.5 M NaCl (3); the excitation wavelength is 333 nm, $T = 25$ °C.

structural parameters of the PIB_{20}-*b*-$PMANa_x$ micelles were found, as is demonstrated below, to be rather sensitive both to pH and ionic strength of the surrounding solution.

3.2. Structure of micelles formed in aqueous solutions of PIB-b-PMAA

In general, macromolecular micelles of a star-like architecture are expected to be generated in solutions of amphiphilic diblock copolymers if the core-forming block is considerably shorter than the corona-forming one. Such assemblies can be characterized by the following structural parameters: the number of macromolecules forming each micelle, i.e. the aggregation number, N_{agg}, the core radius, R_c, and the corona thickness, D_{corona} (Scheme 1). Detailed information about the structure of the macromolecular micelles formed in aqueous solutions of the copolymers used was obtained by means of a combination of SANS and DLS.

3.2.1. Small-angle neutron scattering

The use of SANS allowed us to determine R_c and N_{agg} for various values of the degree of neutralization, α, of the polyelectrolyte blocks of PIB_{20}-*b*-$PMAA_x$ and the ionic strength of the solution. It should be noted, however, that a determination of D_{corona} from the SANS curves presented in our paper is not meaningful because the explored q-range is not sufficient with respect to low values of the scattering vector in order to provide reliable information about the overall size of the PIB_{20}-*b*-$PMAA_x$ micelles. This information, namely, the hydrodynamic radii, R_h, of the formed macromolecular assemblies, was obtained by means of DLS.

The influence of the degree of neutralization, α, on the SANS curves obtained for the salt-free solutions of PIB_{20}-*b*-$PMAA_{100}$ is shown in Fig. 3a. All scattering curves look rather similar and exhibit a correlation peak around 0.013 $Å^{-1}$, corresponding to an average intermicellar distance of 48 nm. In addition to the correlation peak, oscillations at larger q-values are detected: two higher order minima are clearly visible. These arise from the interplay between form factor and structure factor, indicating that the PIB_{20}-*b*-$PMAA_{100}$ micelles are relatively monodisperse. As a general tendency, it is observed that the intensity of the correlation peak decreases by a factor of 2 upon a rise of α from 0.1 up to 1 while the peak position is slightly shifted towards lower q-values. These findings suggest that the aggregation number of the PIB_{20}-*b*-$PMAA_{100}$ micelles becomes smaller with increasing apparent charge of the polyelectrolyte blocks. In the presence of 0.1 M NaCl, a similar decrease in the scattering intensity with increasing values of α is detected (Fig. 3b). However, the correlation peaks observed for this series are much less prominent as compared to the series without the added salt. This latter effect is expected because of the effective screening of the electrostatic repulsion between the PIB_{20}-*b*-$PMAA_{100}$ micelles by small ions (at 0.1 M NaCl, the Debye screening length is about 1 nm).

The obtained SANS curves were quantitatively analyzed on the basis of a core-shell model with constant scattering length densities ρ_c and ρ_0 for the core of the particle and the solvent, respectively. The scattering length density of the

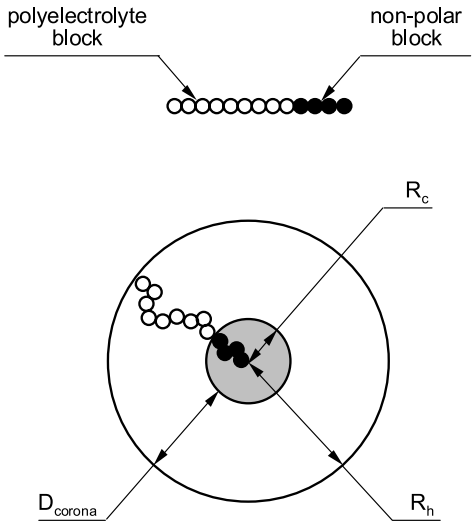

Scheme 1. Schematic representation of a star-like macromolecular micelle in aqueous media.

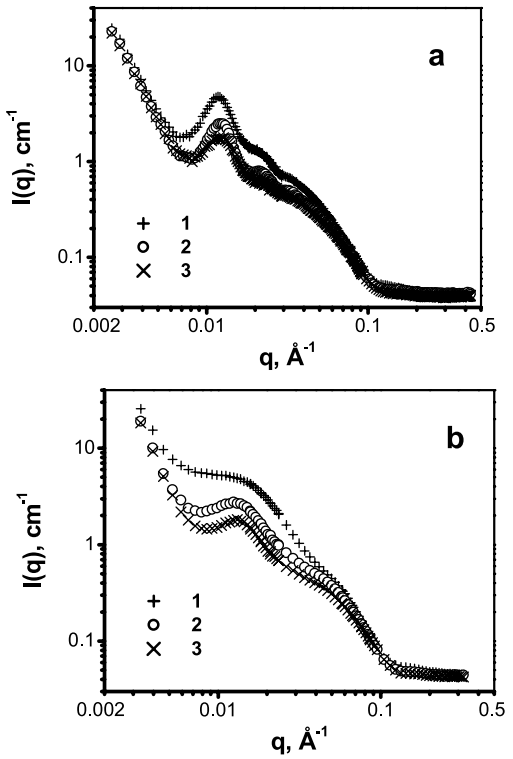

Fig. 3. SANS intensity as a function of the scattering vector, q, for aqueous solutions of PIB_{20}-*b*-$PMAA_{100}$ micelles at $\alpha = 0.1$ (1), 0.5 (2), and 1.0 (3) without added NaCl ([PIB_{20}-*b*-$PMAA_{100}$] = 0.9% (wt)) (a) and at 0.1 M NaCl ([PIB_{20}-*b*-$PMAA_{100}$] = 1.0% (wt)) (b); $T = 25$ °C.

shell, ρ_s, was assumed to vary according to Eq. (1):

$$\rho_s = \rho_1 \left(\frac{r}{R_c} \right)^{-a} \quad \text{for } R_c < r < R_m \tag{1}$$

as was employed previously to describe the scattering for the description of micelles composed of poly(ethylethylene)-*block*-poly(styrene sulfonic acid) diblock copolymer (PEE-*b*-PSSH) [20]. Here, R_m is the maximum micellar radius while a is an exponent describing the radial scattering length density profile in the micellar corona (Scheme 2).

The scattering length density for D_2O was used as $\rho_0 = 63.6 \times 10^9$ cm^{-2}. The value of ρ_c was calculated assuming that the density of the micellar core coincides with that of PIB in the bulk ($\rho_{PIB} = 0.918$ g/cm^3): $\rho_c = -3.3 \times 10^9$ cm^{-2}. The value of ρ_s was evaluated under assumption that the micellar corona is filled with D_2O ($\rho_{D_2O} = 1.105$ g/cm^3) and PMAA (with partial molar volumes of the monomer unit of 59.3 and 39.6 cm^3/mol for protonated and ionized forms, respectively [21,22]).

In the frame of this core-shell model, the scattering intensity, $I(q)$, reads

$$I(q) = {}^1N \int_0^\infty \mathrm{d}R_c f(R_c) P(q, R_c, a, R_m) S(q) \tag{2}$$

where $P(q)$ is the form factor, $S(q)$ is the structure factor, ${}^1N$ is the number density, and $f(R_c)$ is the distribution function of the core radii for which a Schulz distribution was employed [23]. $P(q)$ can be expressed as [20,24]

$$\begin{aligned} \frac{P(q)}{P(0)} = \Bigg\{ \Bigg[& \frac{1}{3} {}_0F_1\left(\frac{3}{2}; -\frac{q^2R_c^2}{4} \right) \\ & - \frac{\rho_1}{\rho_c(3-a)} {}_1F_2\left(\frac{3-a}{2}, \frac{3}{2}, \frac{5-a}{2}, \frac{q^2R_c^2}{4} \right) \\ & + \left(\frac{R_c}{R_m} \right)^{a-3} \frac{\rho_1}{\rho_c(3-a)} \\ & \times {}_1F_2\left(\frac{3-a}{2}, \frac{3}{2}, \frac{5-a}{2}; \frac{q^2R_c^2}{4} \right) \Bigg] \Bigg/ \\ & \Bigg/ \left[\frac{1}{3} + \frac{\rho_1}{\rho_c(3-a)} \left(\left(\frac{R_c}{R_m} \right)^{a-3} - 1 \right) \right] \Bigg\}^2 \end{aligned} \tag{3}$$

where ${}_0F_1(q, R_c)$ and ${}_1F_2(q, R_c, a)$ denote hypergeometric functions. In order to describe $S(q)$, a random-phase approximation for charged spherical particles interacting through a screened Coulomb potential was applied [25].

Since the ratio between the integrated scattering contributions from the core and the corona of the macromolecular micelles is determined by the lengths of hydrophobic and polyelectrolyte blocks of the copolymers used, a combination of ρ_1, R_m, and a represents only two fit parameters. It should be noted, however, that these fit parameters describing the micellar corona have only a minor effect on the resulting values of R_c, which is the key parameter regarding the aggregation number as we deduce it from our analysis. Even a simple core-shell model with a constant scattering length density for the shell would yield similar values for R_c.

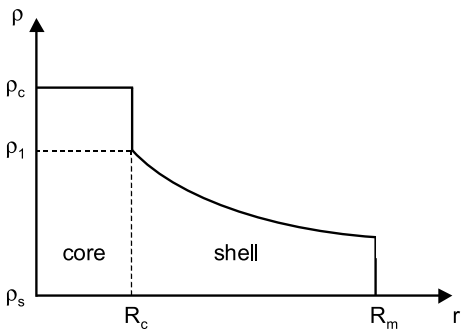

Scheme 2. Scattering length density distribution for the core-shell model.

In this paper, we refrain from a discussion on the structure of the micellar corona on the basis of our SANS results since the parameters extracted result mainly from the parts of the scattering curves at lowest q-values (6–8 points), which obviously are of a limited reliability. Additionally, as we will also see later (from the data obtained by means of DLS), the solutions of macromolecular micelles seem to contain a small fraction of larger particles that would significantly contribute to the scattering at low q-values. Therefore, a detailed information on the structure of the micellar corona from the results obtained by means of SANS appears to be inappropriate. Nevertheless, the values of R_m obtained from the analysis of the scattering curves will be given for an illustrative purpose although we will not consider them in our paper.

The core-shell model described above yields a mean core radius of the macromolecular micelles, R_c, from which their mean aggregation number, N_{agg}, was calculated through the bulk density of PIB and the molecular weight of the PIB block, M_{PIB}, according to the following formula

$$N_{agg} = \frac{4}{3} \pi R_c^3 \frac{\rho_{PIB}}{M_{PIB}} N_A \tag{4}$$

where N_A is the Avogadro's number. The values of R_c and N_{agg} obtained from the data shown in Fig. 3a and b are given in Table 2. One observes that the aggregation number of the PIB_{20}-*b*-$PMAA_{100}$ micelles decreases pronouncedly with increasing degree of neutralization of the PMAA blocks: the values of N_{agg} fall by a factor of 1.6–2.1 upon a rise of α from 0.1 up to 1. Besides, the aggregation numbers of the PIB_{20}-*b*-$PMAA_{100}$ micelles in 0.1 M NaCl are higher (by 1.2–1.5 times) than those obtained for the salt-free system.

It is worthy to note that the values of R_c and N_{agg} determined for the PIB_{20}-*b*-$PMAA_{100}$ micelles are very close to the analogous structural parameters of macromolecular micelles formed in aqueous solutions of a polystyrene-*block*-poly(acrylic acid) diblock copolymer (PS_{20}-*b*-PAA_{80}) with number-average degrees of polymerization of the hydrophobic ($\overline{DP}_n = 20$) and the polyelectrolyte ($\overline{DP}_n = 80$)

Table 2
Structural parameters of the PIB_{20}-*b*-$PMAA_{100}$ micelles for various values of the degree of neutralization of the PMAA blocks without added salt and at 0.1 M NaCl

α	[NaCl] (M)	pH	N_{agg} [a,b]	R_c [a,b] (nm)	R_m [a,b] (nm)	a	p [c]	A [d] (nm^2)	R_h [e] (nm)	D_{corona} [f] (nm)
0.1	0		113[a]	3.7[a]	16.2[a]	0.38	0.19	1.52	–	–
0.5	0		86[a]	3.4[a]	16.5[a]	0.42	0.21	1.69	–	–
1.0	0		71[a]	3.2[a]	16.8[a]	0.45	0.20	1.81	–	–
0.1	0.1	4.9	173[b]	4.3[b]	14.4[b]	0.34	0.18	1.34	16.5	12.2
0.5	0.1	6.3	120[b]	3.8[b]	15.5[b]	0.38	0.22	1.51	21.0	17.2
1.0	0.1	10.0	84[b]	3.4[b]	16.0[b]	0.41	0.19	1.73	22.5	19.1

[a] Measured by means of SANS with the D22 instrument; [PIB_{20}-*b*-$PMAA_{100}$] = 0.9% (wt).
[b] Measured by means of SANS with the D11 instrument; [PIB_{20}-*b*-$PMAA_{100}$] = 1.0% (wt).
[c] Polydispersity index ($p^2 = \langle R^2\rangle/\langle R\rangle^2 - 1$).
[d] Area required for the ionic block to be located at the core–corona interface (calculated according to Eq. (5)).
[e] Measured by means of DLS at the scattering angle 90°; [PIB_{20}-*b*-$PMAA_{100}$] = 0.02% (wt).
[f] Polyelectrolyte corona thickness (calculated according to Eq. (6)).

blocks nearly coinciding with those of PIB_{20}-*b*-$PMAA_{100}$. Indeed, for that copolymer $N_{agg} \approx 100$ and $R_c \approx 4.5$ nm were found [26,27]. In the case of PS_{20}-*b*-PAA_{80}, however, these structural parameters were almost insensitive to a variation of pH or the ionic strength of the surrounding solution, manifesting the 'frozen' nature of the macromolecular micelles formed.

The effect of the ionic strength on the core radius and the aggregation number of the PIB_{20}-*b*-$PMAA_{100}$ micelles at full neutralization of the PMAA blocks is demonstrated in more detail in Fig. 4 and Table 3. An increase in the concentration of NaCl leads to a disappearance of the correlation peak due to the strong electrostatic screening of the intermicellar interaction by small ions. This results in an increase in the values of N_{agg} by ca. 1.5 times upon going from the salt-free system to 1 M NaCl.

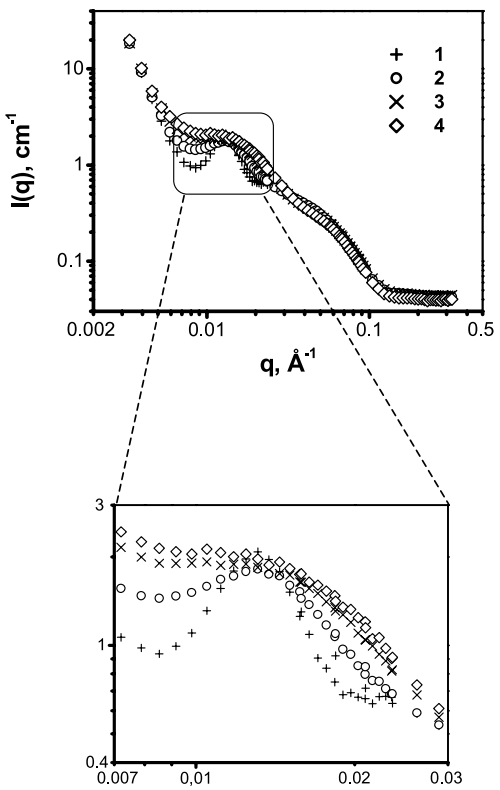

Fig. 4. SANS intensity as a function of the scattering vector, q, for aqueous solutions of PIB_{20}-*b*-$PMAA_{100}$ micelles at full neutralization of the PMAA blocks ($\alpha = 1.0$) without added NaCl (1), at 0.1 M NaCl (2), at 0.5 M NaCl (3), and at 1.0 M NaCl (4); [PIB_{20}-*b*-$PMAA_{100}$] = 1.0% (wt), $T = 25$ °C.

It should be noted that qualitatively similar effects of the ionic strength on the values of R_c and N_{agg} have been observed previously for PEE-*b*-PSSH at salt concentrations exceeding ca. 0.1 M NaCl [20]. A salt-induced increase of the aggregation numbers of macromolecular micelles was also detected for PS-*b*-PANa with relatively short ($\overline{DP}_n = 6, 23$) PS blocks at low concentrations of NaCl (<0.1 M NaCl) while no change of N_{agg} was found with rising ionic strength further (up to 2.5 M NaCl) [28]. However, no salt effect on the values of N_{agg} and R_c was reported for PS_{20}-*b*-PAA_{80} [26]. In contrast to those findings, a decrease in the value of N_{agg} with rising concentration of NaCl (from 0.01 to 0.5 M) was observed for poly(*tert*-butylstyrene)-*block*-poly(sodium styrenesulfonate) (P*t*BS-*b*-PSSNa) [29]. Finally, it might be noted that the increase of the

Table 3
Effect of the concentration of NaCl on the structural parameters of the PIB_{20}-*b*-$PMAA_{100}$ micelles at full neutralization of the PMAA blocks ($\alpha = 1.0$)

[NaCl] (M)	N_{agg} [a]	R_c [a] (nm)	R_m [a] (nm)	a	p [b]	A [c] (nm^2)	R_h [d] (nm)	D_{corona} [e] (nm)
0	71	3.2	16.8	0.45	0.20	1.81	–	–
0.1	84	3.4	16.0	0.41	0.19	1.73	22.5	19.1
0.5	89	3.5	15.8	0.40	0.23	1.73	19.5	16.0
1.0	106	3.7	15.2	0.37	0.22	1.62	18.5	14.8

[a] Measured by means of SANS with the D11 instrument; [PIB_{20}-*b*-$PMAA_{100}$] = 1.0% (wt).
[b] Polydispersity index ($p^2 = \langle R^2\rangle/\langle R\rangle^2 - 1$).
[c] Area required for the ionic block to be located at the core–corona interface (calculated according to Eq. (5)).
[d] Measured by means of DLS at the scattering angle 90°; [PIB_{20}-*b*-$PMAA_{100}$] = 0.02% (wt).
[e] Polyelectrolyte corona thickness (calculated according to Eq. (6)).

aggregation numbers with increasing ionic strength is commonly encountered for low molecular weight ionic surfactants.

For PIB_{20}-*b*-$PMAA_{280}$ and PIB_{20}-*b*-$PMAA_{425}$ diblock copolymers, the effect of the ionic strength on the structural parameters of the micelles is qualitatively similar. As is seen from a comparison of the scattering curves given in Fig. 5a and b, the scattering intensities obtained for solutions of the PIB_{20}-*b*-$PMAA_x$ micelles at 0.1 M NaCl (Fig. 5b) demonstrate a clear tendency to be higher as compared to those for the corresponding salt-free systems (Fig. 5a), indicating that micelles with larger aggregation numbers are formed in the presence of NaCl. The values of R_c and N_{agg} evaluated from these SANS curves are given in Table 4. The aggregation numbers were found to considerably increase (by 1.7–3.2 times) with rising ionic strength, this increase becoming more pronounced for increasing length of the PMAA blocks. At the same time, no distinct dependence of these structural parameters on the length of the PMAA block is detected, although a decrease in the aggregation number of macromolecular micelles with increasing length of a polyelectrolyte block was predicted theoretically and observed previously [3].

The effects of the degree of neutralization of the PMAA blocks and the ionic strength on the values of R_c and N_{agg} of the PIB_{20}-*b*-$PMAA_x$ micelles can be reasonably explained on a basis of a simple packing model that takes into account an area, *A*, required for each ionic block to be located at the

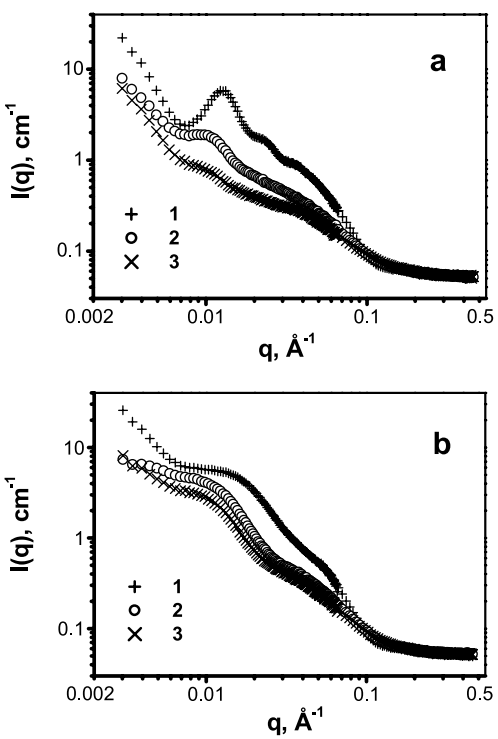

Fig. 5. SANS intensity as a function of the scattering vector, *q*, for aqueous solutions of PIB_{20}-*b*-$PMAA_x$ micelles with $x = 100$ (1), 280 (2), and 425 (3) at $\alpha = 0.1$ without added of NaCl (a) and at 0.1 M NaCl (b); [PIB_{20}-*b*-$PMAA_x$] = 0.9% (wt), $T = 25$ °C.

Table 4
Structural parameters of the PIB_{20}-*b*-$PMAA_x$ micelles at the constant degree of neutralization $\alpha = 0.1$ of the PMAA blocks without added salt and at 0.1 M NaCl

x	[PIB_{20}-*b*-$PMAA_x$] (mM)	[NaCl] (M)	N_{agg} [a]	R_c [a] (nm)	R_m [a] (nm)	*a*	p [b]
100	1.0	0	113	3.7	16.2	0.38	0.19
280	0.4	0	171	4.3	24.5	0.35	0.23
425	0.3	0	146	4.1	31.2	0.33	0.24
100	1.0	0.1	187	4.4	17.4	0.37	0.22
280	0.4	0.1	449	5.9	23.8	0.33	0.23
425	0.3	0.1	461	6.0	33.0	0.30	0.22

[a] Measured by means of SANS with the D22 instrument; [PIB_{20}-*b*-$PMAA_x$] = 0.9% (wt).
[b] Polydispersity index ($p^2 = \langle R^2\rangle/\langle R\rangle^2 - 1$).

core–corona interface. This parameter is the equivalent of the head group area of low molecular weight surfactants. A rise in α or the decrease in the concentration of NaCl are expected to result in a concomitant increase of an apparent charge of the PMAA blocks and therefore strengthens the electrostatic repulsion among them within the micellar coronas. As a consequence, the micelles formed at higher values of α or lower concentrations of NaCl are supposed to be characterized by larger values of *A* than those formed at lower values of α or higher concentrations of NaCl.

This explanation is directly confirmed by the obtained experimental data. Indeed, one can easily evaluate *A* as

$$A = 4\pi R_c^2/N_{agg} \quad (5)$$

The values of *A* evaluated for the PIB_{20}-*b*-$PMAA_{100}$ micelles are presented in Tables 2 and 3. They increase with rising degree of neutralization of the PMAA blocks and decreasing ionic strength of the solution, this being realized by the formation of the PIB_{20}-*b*-$PMAA_{100}$ micelles with lower values of R_c and N_{agg}. Additionally, the values of *A* are, in general, rather small: they change from ca. 1.3 up to ca. 1.8 nm^2 upon the variation of the conditions of the surrounding medium, thereby indicating a very high grafting density of the PMAA blocks at the core–corona interface. It is worthy to mention that these values are only by a factor 2–3 higher than the head group areas typically observed for low molecular weight ionic surfactants.

The sensitivity of N_{agg} to the degree of neutralization of the PMAA blocks and the ionic strength of the solution seems to suggest the 'dynamic' nature of the PIB_{20}-*b*-$PMAA_x$ micelles. However, additional experiments, e.g. similar to those described in Refs. [30–32] on fluorescence energy transfer, are required to clarify this point. Such experiments are planned to be carried out in future studies.

3.2.2. Dynamic light scattering

Further information on the structure of the PIB_{20}-*b*-$PMAA_x$ micelles was obtained by means of DLS. Fig. 6a shows a typical set of normalized correlation functions obtained for solutions of the PIB_{20}-*b*-$PMAA_{100}$ micelles at

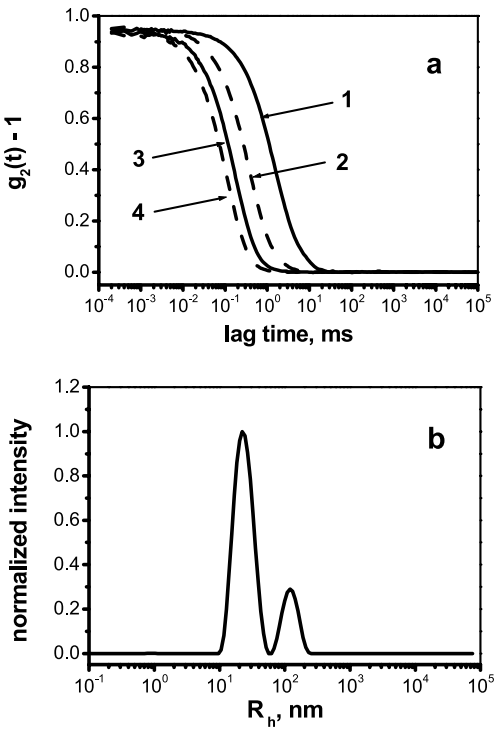

Fig. 6. Normalized correlation functions obtained for the solution of the PIB_{20}-*b*-$PMAA_{100}$ micelles at full neutralization of the PMAA blocks ($\alpha = 1.0$) at different scattering angles 30° (1), 60° (2), 90° (3), and 120° (4) (a) and intensity distribution of hydrodynamic radii of the micelles at a scattering angle of 90° (b); [PIB_{20}-*b*-$PMAA_{100}$] $= 2 \times 10^{-5}$ M, 0.1 M NaCl, $T = 25$ °C.

full neutralization of the PMAA blocks and 0.1 M NaCl for four different scattering angles. The result of an analysis of the correlation function detected at 90° by the CONTIN algorithm is shown in Fig. 6b as an intensity distribution $z(R_h)$ of hydrodynamic radii of the PIB_{20}-*b*-$PMAA_{100}$ micelles. This distribution is bimodal: species with R_h of 22.5 and 130 nm are detected in the system. The values of R_h obtained for the small species are nearly independent of the scattering angle, suggesting their spherical morphology. These small species are considered to be common macromolecular micelles. In contrast, the values of R_h obtained for the large species show a pronounced angular dependence. These much larger objects might be associated either with micellar clusters or vesicles as was proposed earlier for PIB_{70}-*b*-$PMAA_x$ ($x = 52, 70$) and PIB_{134}-*b*-$PMAA_x$ ($x = 145, 288$) [5]. Although these large species give a considerable contribution to the intensity of scattered light, their weight-average or even number-average fraction seems to be vanishing (less than a few percent by weight) and therefore their presence in our systems may be neglected.

The effects of the degree of neutralization of the PMAA blocks and the ionic strength on the values of R_h of the PIB_{20}-*b*-$PMAA_{100}$ micelles are shown in Tables 2 and 3. As expected, these values increase upon a rise of α or a decrease in the concentration of NaCl. The obvious reason for that is an increasing apparent charge of the PMAA blocks, leading to their stretching. It should be noted that a similar effect, i.e. an expansion of the polyelectrolyte corona with decreasing ionic strength, was also reported earlier for PEE-*b*-PSSH [20] and PS_{20}-*b*-PAA_{80} [33]. The increase of the radius of gyration (R_g) of macromolecular micelles and their R_h with decreasing concentration of NaCl was also found for P*t*BS-*b*-PSSNa [29] while no considerable influence of the ionic strength on the values of R_g was observed for micelles formed in aqueous solutions of PS-*b*-PANa [28].

Since the values of R_c are known, one can evaluate a thickness of the polyelectrolyte corona by subtracting the contribution of the micellar core to R_h

$$D_{corona} = R_h - R_c \quad (6)$$

The values of D_{corona} evaluated at different values of α and concentrations of NaCl are also given in Tables 2 and 3. It is remarkable that D_{corona} ranges from 50 to 75% of the contour length of the PMAA blocks ($L_S = \overline{DP}_{PMAA} l_0 = 25$ nm for PIB_{20}-*b*-$PMAA_{100}$, assuming the contour length of the monomer unit, l_0, to be 0.25 nm), indicating that the polyelectrolyte blocks are rather stretched in the micellar corona. A similar conclusion was also drawn previously in some other papers [20,26–28,34,35].

3.3. Interpolyelectrolyte complexes of PIB-b-PMANa micelles

Since the coronas of the formed copolymer micelles are built up from the PMAA blocks, such micelles are naturally expected to interact with oppositely charged macromolecules, generating interpolyelectrolyte complexes (IPECs). Although IPECs formed by oppositely charged linear polyions were thoroughly investigated during the last decades (cf. the reviews [36–38]), so far the interaction of micelles of ionic amphiphilic block copolymers with oppositely charged polyelectrolytes has received only little attention both experimentally [39] and theoretically [40]. In this paper, we consider the interpolyelectrolyte complexation of PIB_{20}-*b*-$PMANa_x$ micelles, whose PMAA blocks are fully neutralized by NaOH, with quaternized poly(4-vinylpyridine), PVP·EtBr, and describe the structure and some properties of the IPECs resulting from this complexation.

3.3.1. Turbidimetry

On addition of the solution of PVP·EtBr to solutions of the PIB_{20}-*b*-$PMANa_x$ micelles, no macroscopic phase separation is observed until the charge ratio of the polyelectrolytes, $Z = [+]/[-]$, exceeds a certain value, Z_M. The values of Z_M were found to range from ca. 0.4 up to ca. 0.6, being dependent on the length of the PMANa block and the concentration of NaCl. When $Z < Z_M$, the mixtures of the PIB_{20}-*b*-$PMANa_x$ micelles and PVP·EtBr remain homogeneous. Such homogeneous mixtures were examined

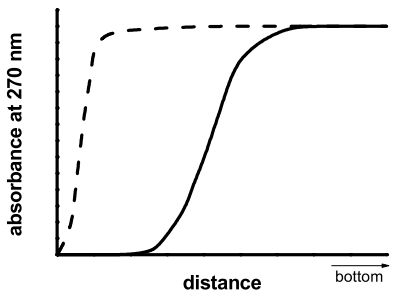

Fig. 7. Sedimentation profiles detected after 15 min for a mixture of PIB_{20}-*b*-$PMANa_{100}$ and PVP·EtBr with $Z = [+]/[-] = 0.4$ (solid line) and for the reference solution of PVP·EtBr (dashed line); $[PIB_{20}$-*b*-$PMANa_{100}] = 2 \times 10^{-5}$ M; pH 9 (0.01 M TRIS), 0.2 M NaCl, $T = 25$ °C.

by means of analytical ultracentrifugation and fluorescence spectroscopy.

3.3.2. Analytical ultracentrifugation

As a typical example, Fig. 7 shows one of the sedimentation patterns obtained for the mixture of PIB_{20}-*b*-$PMANa_{100}$ and PVP·EtBr with $Z = 0.4$ in the scanning mode at $\lambda = 270$ nm. At this wavelength, the cationic polyelectrolyte absorbs light while the copolymers possess nearly no absorbance. Only one type of species is detected in the pattern, their sedimentation coefficient, $S \cong 25$ Sv, being considerably higher than the sedimentation coefficient of the individual PVP·EtBr, $S_{PVP\cdot EtBr} \cong 1.5-2$ Sv. Thus, these species can be considered as particles of the water-soluble IPEC resulting from the interaction of PIB_{20}-*b*-$PMANa_x$ micelles with PVP·EtBr, all polycations being incorporated in such particles and evenly distributed among them.

3.3.3. Fluorescence spectroscopy

The data presented in Table 5 evidence that the values of I_1/I_3 for solutions of the IPECs are lower than those obtained for the pure solvent ($I_1/I_3 \cong 1.85$), indicating that the formed IPEC species solubilize pyrene. The reference experiments carried out under the same conditions with solutions of the corresponding linear anionic homopolyelectrolyte, PMANa ($\overline{DP}_n = 400$), and with solutions of the IPECs formed upon the interaction between PMANa and PVP·EtBr show no solubilization of pyrene: the values of I_1/I_3 for such solutions are nearly equal to 1.85. These findings indicate that the IPEC particles formed upon mixing solutions of the PIB_{20}-*b*-$PMANa_x$ micelles and PVP·EtBr, as well as the pure macromolecular micelles, contain hydrophobic cores consisting of the PIB blocks, pyrene being solubilized by such cores.

At the same time, the values of I_1/I_3 for solutions of IPECs are higher than those obtained for the corresponding solutions of the pure PIB_{20}-*b*-$PMANa_x$ micelles. Moreover, the fluorescence intensity of pyrene in solutions of IPECs is distinctly lower than that measured under the same conditions in solutions of the corresponding copolymers (Table 5). The above differences could be accounted for quenching of the fluorescence probe emission by pyridinium groups of the polycations located in the vicinity of the PIB cores. In such a case, a contribution of pyrene molecules not being solubilized by the IPEC species, that is, existing in the polar environment, to the overall fluorescence spectrum of pyrene is naturally increased, thereby increasing the I_1/I_3 ratio.

Fig. 8 shows the dependence of the relative fluorescence intensity of solutions of IPECs resulting from the interaction of PIB_{20}-*b*-$PMANa_{100}$ micelles with PVP·EtBr, $I_{IPEC}/I_{PIB\text{-}b\text{-}PMANa}$, on Z. The values of $I_{IPEC}/I_{PIB\text{-}b\text{-}PMANa}$ steeply fall with rising content of PVP·EtBr, approaching a limiting value already at $Z = 0.1$. The observed tendency suggests that the polycations in the formed IPEC species prefer to be located in the vicinity of its PIB core.

Thus, the obtained results suggest that the IPEC species can be considered as a peculiar onion-like complex micelle whose hypothetical architecture is schematically depicted in

Table 5
Values of I_1/I_3 for solutions of PIB_{20}-*b*-$PMANa_x$ and for solutions of IPECs with $Z = [+]/[-] = 0.4$ as well as values of the relative fluorescence intensity $I_{IPEC}/I_{PIB\text{-}b\text{-}PMANa}$ for solutions of the IPECs; $[PIB_{20}$-*b*-$PMANa_x] = 7 \times 10^{-6}$ M; 0.05 M NaCl, 0.01 M TRIS

x	PIB_{20}-*b*-$PMANa_x$ micelles	IPEC	
	I_1/I_3	I_1/I_3	$I_{IPEC}/I_{PIB\text{-}b\text{-}PMANa}$[a]
100	1.60	1.73	0.48
280	1.60	1.72	0.62
425	1.68	1.73	0.48

[a] I_{IPEC} is the fluorescence intensity of pyrene in the solution of IPEC while $I_{PIB\text{-}b\text{-}PMANa}$ is the fluorescence intensity of pyrene in the reference solution of PIB_{20}-*b*-$PMANa_x$; I_{IPEC} and $I_{PIB\text{-}b\text{-}PMANa}$ were measured at the third vibrational band of the fluorescence spectrum of pyrene; the excitation wavelength is 333 nm.

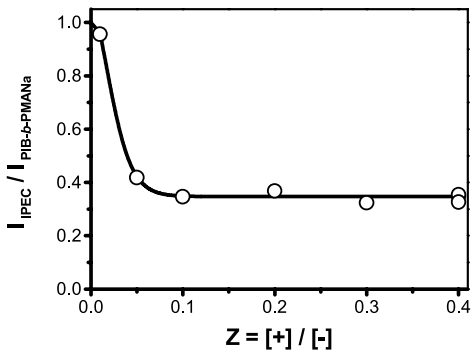

Fig. 8. Dependence of the relative fluorescence intensity $I_{IPEC}/I_{PIB\text{-}b\text{-}PMANa}$ of the IPEC solutions on the charge ratio $Z = [+]/[-]$; $[PIB_{20}$-*b*-$PMANa_{100}] = 2 \times 10^{-5}$ M; pH 9 (0.01 M TRIS), 0.05 M NaCl, $T = 25$ °C; the excitation wavelength is 333 nm; I_{IPEC} (I_{IPEC} is the fluorescence intensity of the solution of IPEC) and $I_{PIB\text{-}b\text{-}PMANa}$ ($I_{PIB\text{-}b\text{-}PMANa}$ is the fluorescence intensity of the reference solution of PIB_{20}-*b*-$PMANa_{100}$) were measured at the third vibrational band of the fluorescence spectrum of pyrene.

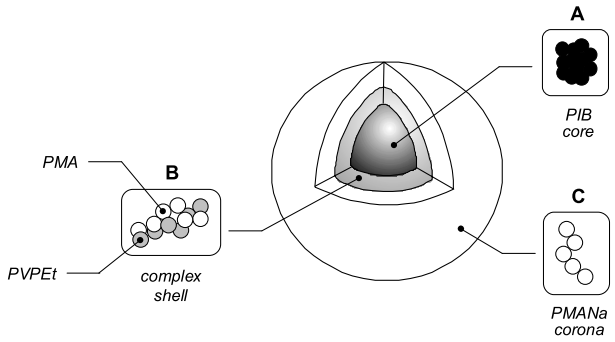

Scheme 3. Hypothetical architecture of a particle of the micellar IPEC.

Scheme 3. Each species is assumed to consist of the PIB core (A) surrounded by a shell (B) assembled from the interacting oppositely charged polyelectrolyte fragments and the ionic corona (C) formed by fragments of the PMANa blocks not involved in the interpolyelectrolyte complexation. The polyelectrolyte corona apparently stabilizes the whole complex micelle in aqueous media.

3.3.4. Small-angle neutron scattering

Fig. 9 shows the SANS curves obtained for pure PIB_{20}-*b*-$PMANa_{100}$ micelles and the IPEC species formed upon their interaction with PVP·EtBr. A much higher scattering intensity and a larger slope at intermediate q-values are observed in the latter case, both indicating an increase in size of the micellar core as compared to the pure PIB_{20}-*b*-$PMANa_{100}$ micelles. At the same time, the position of the correlation peak does not change, i.e. the interparticle spacing remains constant.

The obtained results appear to be in a good agreement with the proposed above architecture of the water-soluble micellar IPEC (Scheme 3). Indeed, the observed effects could be explained if we assume a relatively dense complex shell to be assembled from interacting oppositely charged polyelectrolyte fragments around the PIB core. It is important to note that under the given contrast condition we cannot separate in a meaningful way the scattering contributions from the core and the shell of the formed IPEC species.

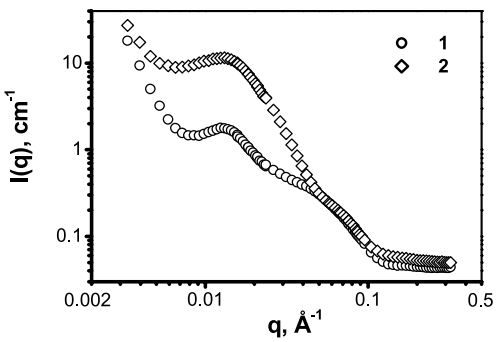

Fig. 9. SANS intensity as a function of the scattering vector, q, for solutions of the PIB_{20}-*b*-$PMANa_{100}$ micelles (1) and their IPEC at $Z = 0.4$ (2); [PIB_{20}-*b*-$PMANa_{100}$] = 1.0% (wt); pH 9 (0.01 M TRIS), 0.1 M NaCl, T = 25 °C.

For a quantitative analysis of the scattering curve obtained for the IPEC species (Fig. 9, curve 2), we consider their hydrophobic cores to contain PIB and the corresponding amount of stoichiometric, that is, including the opposite charges in the equivalent ratio IPEC, whose density was taken to be of 1.15 g/cm^3. Under this assumption, the average scattering length density ρ_c for the complex hydrophobic core is evaluated to be of 11.9×10^9 cm^{-2}. The analysis of the scattering curve on the basis of the core-shell model described above (Scheme 2) yields values of R_c and N_{agg} for the IPEC species (Table 6). It is remarkable that their aggregation number is only slightly larger (~5%, i.e. within the error bar of this experiment which we estimate to be about 10%) than that of the pure PIB_{20}-*b*-$PMANa_{100}$ micelles, whereas the core radius increases considerably (by a factor of 2).

3.3.5. Dynamic light scattering

Additionally, the value of R_h for the IPEC species was found to be measurably but not pronouncedly lower than that characteristic for the pure PIB_{20}-*b*-$PMANa_{100}$ micelles (Table 6). This finding also seems to suggest that polycations interacting with the copolymer micelles prefer to penetrate deeply inside their coronas via polyion exchange reactions (cf. review [37]) in order to be finally localized in a vicinity of the PIB cores. The observed decrease in R_h of the IPEC species compared to the pure PIB_{20}-*b*-$PMANa_{100}$ micelles indicates a collapse of some fragments of the formerly stretched PMANa blocks due to their interaction with PVP·EtBr.

4. Conclusions

The experimental results reported in this work demonstrate that the ionic amphiphilic diblock copolymers PIB_{20}-*b*-$PMAA_x$ (x = 100, 280, 425) self-assemble in aqueous media to form micelles, the values of the molar cmc being nearly independent of the length of the polyelectrolyte block as well as of pH (in the range 6–9) and ionic strength of the surrounding medium (at least, up to 0.5 M NaCl). The aggregation numbers of the formed copolymer micelles are sensitive to variations of pH and ionic strength: a decrease of pH or an increase in the

Table 6
Structural parameters of the PIB_{20}-*b*-$PMANa_{100}$ micelles and the IPEC species ($Z = [+]/[-] = 0.4$); 0.1 M NaCl, 0.01 M TRIS

PIB_{20}-*b*-$PMANa_{100}$ micelles			IPEC		
N_{agg} [a]	R_c [a] (nm)	R_h [b] (nm)	N_{agg} [a]	R_c [a] (nm)	R_h [b] (nm)
84	3.4	22.5	88	6.3	19.0

[a] Measured by means of SANS with the D11 instrument; [PIB_{20}-*b*-$PMANa_{100}$] = 1.0% (wt).
[b] Measured by means of DLS at the scattering angle 90°; [PIB_{20}-*b*-$PMANa_{100}$] = 0.02% (wt).

concentration of NaCl leads to a distinct rise in the values of this structural parameter. The hydrodynamic radii of the formed copolymer micelles increase at higher pH or decreasing ionic strength, these effects are thought to be mainly due to an expansion of the micellar coronas upon the rising apparent charge of the PMAA blocks.

The formed macromolecular micelles interacting with oppositely charged polyelectrolytes form a novel type of water-soluble IPECs in which the polyelectrolyte component of the original micelles apparently plays a lyophilizing part. The IPEC species is hypothesized to be a complex micelle consisting of a two-phase hydrophobic nucleus formed by a polyisobutylene core surrounded by a shell of coupled oppositely charged polyelectrolyte fragments and an ionic corona formed by fragments of PMANa blocks not involved in the interpolyelectrolyte complexation.

Acknowledgements

This research was supported by the Deutsche Forschungsgemeinschaft, the Russian Foundation for Basic Research (project no. 03-03-32511), and INTAS (project no. IR-97-0278). I. Grillo (ILL), X. André, N. Martínez-Castro, and G. Jutz (Universität Bayreuth) are gratefully acknowledged for help with the SANS measurements.

References

[1] Selb J, Gallot Y. In: Goodman I, editor. Developments in block copolymers, vol. 2. London: Elsevier; 1985. p. 27–96.
[2] Moffitt M, Khougaz K, Eisenberg A. Acc Chem Res 1996;29:95–102.
[3] Förster S, Abetz V, Müller AHE. Adv Polym Sci 2003; in press.
[4] Feldthusen J, Iván B, Müller AHE. Macromolecules 1998;31:578–85.
[5] Schuch H, Klingler J, Rossmanith P, Frechen T, Gerst M, Feldthusen J, Müller AHE. Macromolecules 2000;33:1734–40.
[6] Harada A, Kataoka K. Macromolecules 1995;28:5294–9.
[7] Kabanov AV, Bronich TK, Kabanov VA, Yu K, Eisenberg A. Macromolecules 1996;29:6797–802.
[8] Cohen Stuart MA, Besseling NAM, Fokkink RG. Langmuir 1998;14:6846–9.
[9] Harada A, Kataoka K. Langmuir 1999;15:4208–12.
[10] Bronich TK, Nguen HK, Eisenberg A, Kabanov AV. J Am Chem Soc 2000;122:8339–43.
[11] Gohy J-F, Varshney SK, Antoun S, Jérôme R. Macromolecules 2000;33:9298–305.
[12] Pergushov DV, Remizova EV, Feldthusen J, Zezin AB, Müller AHE, Kabanov VA. J Phys Chem (B) 2003;107:8093–6.
[13] Wilhelm M, Zhao C-L, Wang Y, Xu R, Winnik MA, Mura J-L, Riess G, Croucher MD. Macromolecules 1991;24:1033–40.
[14] Astafieva I, Zhong XF, Eisenberg A. Macromolecules 1993;26:7339–52.
[15] Astafieva I, Khougaz K, Eisenberg A. Macromolecules 1995;28:7127–34.
[16] Ghosh RE, Egelhaaf SU, Rennie AR. A computing guide for small-angle scattering experiments. ; 1998. ILL98GH14T.
[17] Kalyanasundaram K, Thomas JK. J Am Chem Soc 1977;99:2039–44.
[18] Dong DC, Winnik MA. Photochem Photobiol 1982;35:17–21.
[19] Corrin ML, Harkins WD. J Am Chem Soc 1947;69:684–92.
[20] Förster S, Hermsdorf N, Böttcher C, Lindner P. Macromolecules 2002;35:4096–105.
[21] Tondre C, Zana R. J Phys Chem 1972;70:3451–6.
[22] Ikegami A. Biopolymers 1968;6:431–8.
[23] Schulz GV. Z Phys Chem B 1939;43:25–33.
[24] Förster S, Burger C. Macromolecules 1998;31:879–91.
[25] Baba-Ahmed L, Benmouna M, Grimson MJ. Phys Chem Liq 1987;16:235–40.
[26] Groenewegen W, Egelhaaf SU, Lapp A, van der Maarel JRC. Macromolecules 2000;33:3283–93.
[27] Groenewegen W, Lapp A, Egelhaaf SU, van der Maarel JRC. Macromolecules 2000;33:4080–6.
[28] Khougaz K, Astafieva I, Eisenberg A. Macromolecules 1995;28:7135–47.
[29] Guenoun P, Davis HT, Tirrell M, Mays JW. Macromolecules 1996;29:3965–9.
[30] Creutz S, Van Stam J, Antoun S, De Schryver FC, Jérôme R. Macromolecules 1997;30:4078–83.
[31] Creutz S, Van Stam J, De Schryver FC, Jérôme R. Macromolecules 1998;31:681–9.
[32] Van Stam J, Creutz S, De Schryver FC, Jérôme R. Macromolecules 2000;33:6388–95.
[33] Van der Maarel JRC, Groenewegen W, Egelhaaf SU, Lapp A. Langmuir 2000;16:7510–9.
[34] Guenoun P, Muller F, Delsanti M, Auvray L, Chen YJ, Mays JW, Tirrell M. Phys Rev Lett 1998;81:3872–5.
[35] Burguière C, Chassenieux C, Charleux B. Polymer 2003;44:509–18.
[36] Smid J, Fish D. In: Mark HF, Bikales NM, Overberger CG, Menges G, editors. Encyclopedia of polymer science and engineering, vol. 11. New York: Wiley; 1988. p. 720–39.
[37] Kabanov VA. In: Dubin P, Bock J, Davies RM, Schulz DN, Thies C, editors. Macromolecular complexes in chemistry and biology. Berlin: Springer; 1994. p. 151–74.
[38] Philipp B, Dautzenberg H, Linow KJ, Koetz J, Dawydoff W. Prog Polym Sci 1989;14:91–172.
[39] Talingting MR, Voigt U, Munk P, Webber SE. Macromolecules 2000;33:9612–9.
[40] Simmons C, Webber SE, Zhulina EB. Macromolecules 2001;34:5053–66.